

RSC Advances



This is an *Accepted Manuscript*, which has been through the Royal Society of Chemistry peer review process and has been accepted for publication.

Accepted Manuscripts are published online shortly after acceptance, before technical editing, formatting and proof reading. Using this free service, authors can make their results available to the community, in citable form, before we publish the edited article. This *Accepted Manuscript* will be replaced by the edited, formatted and paginated article as soon as this is available.

You can find more information about *Accepted Manuscripts* in the [Information for Authors](#).

Please note that technical editing may introduce minor changes to the text and/or graphics, which may alter content. The journal's standard [Terms & Conditions](#) and the [Ethical guidelines](#) still apply. In no event shall the Royal Society of Chemistry be held responsible for any errors or omissions in this *Accepted Manuscript* or any consequences arising from the use of any information it contains.

ARTICLE

Single step hydrothermal synthesis of hierarchical TiO₂ microflowers with radially assembled nanorods for enhanced photovoltaic performance

Cite this: DOI: 10.1039/x0xx00000x

Received 00th January 2012,

Accepted 00th January 2012

DOI: 10.1039/x0xx00000x

www.rsc.org/Pallavi B. Patil,^a Sawanta S. Mali,^c Vijay V. Kondalkar,^a Nita B. Pawar,^a Kishorkumar V. Khot,^a Chang K. Hong,^c Pramod S. Patil,^b Popatrao N. Bhosale^{a*}

Abstract

Herein, 3D hierarchical TiO₂ microflowers with well faceted profile and high crystallinity were successfully obtained via surfactant directed single step facile hydrothermal technique. TiO₂ thin films were subjected to different characterization techniques such as UV-Vis-NIR spectrometry, X-ray diffraction (XRD), High resolution transmission electron microscopy (HRTEM), Scanning electron microscopy (SEM) and X-ray photoelectron spectroscopy (XPS) for their optical, structural, morphological and compositional analysis. The morphological characterization indicated that microflowers are made from numerous nanorods growing homocentrically. The length, diameter and degree of aggregation of nanorod increase rapidly and become aggregated with increase in concentration of CTAB. The effect of CTAB concentration on microstructure and photoelectric properties of solar cell i.e. open circuit voltage (V_{oc}), short circuit current density (J_{sc}) and photoelectric conversion efficiency ($\eta\%$) were investigated under UV illumination. The synthesized 3D hierarchical microflowers can act as a scattering overlayer and 1D nanorod underlayer. 1D nanorod can accelerate the movement of electron in one direction, while microflowers can scatter the light and can enhance the cell performance by light harvesting. The effective improvement in the photoconversion efficiency was observed and lies in the range 0.23% to 3.72%.

Introduction

Over the past few years, many kinds of solar cells have been designed and fabricated [1]. Titanium Oxide (TiO₂) got intensive interest due to its applications in, lithium ion batteries [2], photocatalysis [3-4], self cleaning devices [5], Quantum dot / Dye sensitized solar cell (QD/DSSC) [6-12] and tissue engineering scaffolds [13]. In recent years, the control over morphology of metal oxide has attracted great attention. TiO₂ with different morphology such as nanoparticle, nanotube, nanorods, nanobelts, microsphere, nanofibers have been prepared by sol-gel method [14-16], electrochemical anodic oxidation [17, 18], hydrothermal method [19-24], electrospinning method [25], chemical vapour deposition [26, 27] and spray pyrolysis technique [28]. For instance, the aforesaid 1D nanostructure possess low internal surface area resulting poor light harvesting and low conversion efficiency. One cure for this problem is to synthesize branched nanostructure or to synthesize 3D nanostructure, which provides large internal surface area for better light harvesting for better conversion efficiency.

Recently, considerable results were achieved with self assembled 1D nanostructure into 3D hierarchical architecture because longer pathway for photon transports, large number of active sites, unique

multidimensional hybrid morphology and enhanced light harvesting property.[29] Till now, extensive research has been conducted to improve PEC performances with scattering layers in the field of materials chemistry, Y.C. Park et.al. synthesized mesoporous TiO₂ as a scattering layer by two step synthesis process with highest efficiency 9.37% [30]. J. Jiang et.al. demonstrated novel microemulsion-based spherical multihollow TiO₂ nanostructures by two step synthesis which acts as scattering overlayer and Degussa P25 underlayer gives 2.33% conversion efficiency [31]. 9.43% energy conversion efficiency based on DSSC is achieved by H. J. Koo et.al. by preparing a nano- embossed hollow spherical TiO₂ layer on 20 nm thick TiO₂ particulate film [32]. S. R. Gajjela et.al. reported a photoconversion efficiency 10.63% for 1 Sun MPT while 10.84% for 0.16 Sun MPT based on DSSC after surface treatment by 40mM TiCl₄ (aq.) solution and screen printed by MPT or NPT of TiO₂ [33]. H. Pang et.al. demonstrated the visible range scattering effect of the submicron-sized hollow TiO₂ spheres and a bilayered photoelectrode constructed by coating approximately 10 μ m thick layer of the hollow TiO₂ on top of approximately 10 μ m layer of commercial P25 TiO₂ which gives conversion efficiency 7.48% [34]. All above results based on two step synthesis of double layered/bilayered TiO₂ for effective solar cell performance.

Herein we design a novel hierarchical multidimensional hybrid structured TiO₂ photoanode by facile one step hydrothermal method. In preliminary the TiO₂ thin films were synthesized without CTAB surfactant (sample S₁) and in order to investigate the effect of CTAB surfactant on morphology, the concentration of CTAB was varied from 0.025-0.15% (S₂-S₅). This shows enhancement in the photoconversion efficiency from 0.23-3.72% by providing the direct pathway for photogenerated electrons to flow through TiO₂/ FTO interface. There is formation of TiO₂ microflowers which is act as scattering overlayer and nanorod underlayer. Therefore it is significant to fabricate hierarchical TiO₂ photoanode with both high light harvesting and good electron transferring property.

Experimental Procedure

The chemical reagents used for the synthesis of hierarchical multidimensional hybrid structured TiO₂ microflowers were commercially available titanium isopropoxide (TTIP), hydrochloric acid (HCl), ethylene glycol (EG) and cetyl trimethyl ammonium bromide (CTAB) as a Ti- precursors, acid medium, cosolvent and surfactant respectively. To prepare TiO₂ thin films a mixture of 0.04 M TTIP, 3M HCl and EG (TTIP: EG= 1:1) were used as a starting material, mixed with appropriate volume and stirred for 30 min. To this mixture different percentage of CTAB were added, again stirred for another 10 min to improve its homogeneity. The mixed solution was transfer into Teflon lined stainless steel autoclave containing FTO with conducting side facing up. Subsequently, autoclave was maintained at 160°C for 6 hr, cool the autoclave naturally. Then TiO₂ thin film removed from autoclave washed with water dried in air and annealed at 400°C for 1 hr.

In order to investigate the effect of CTAB on the morphology and photoelectrochemical performance the concentration of CTAB was varied from 0.00%, 0.025%, 0.05%, 0.1% and 0.15% samples designated as S₁, S₂, S₃, S₄ and S₅ respectively. The reaction temperature and time is kept constant as, 160°C and 6 hr respectively for all deposition.

Characterization

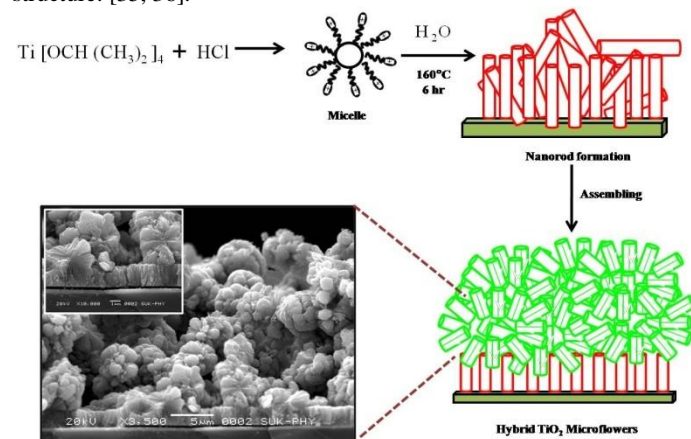
The crystal structure of the samples were analyzed by X-ray powder diffraction (XRD) with Rigaku, D/MAX Ultima III XRD spectrometer (Japan) using CuK α radiation ($\lambda = 1.54 \text{ \AA}$) in 2θ range 20 - 80°. The morphology and microstructure were examined by using scanning electron microscope (SEM) model (SEM, JEOL-6360) equipped with energy dispersive X-ray spectroscopy (EDS). The elemental composition and valance state of elements were examined by X-ray photoelectron spectroscopy (XPS) using a VG Multilab 2000- Thermo Scientific, USA, K-alpha. UV-Vis-NIR absorbance spectra were measured using a Shimadzu UV- 1800 (Japan) in the wavelength range 350-1100 nm. Crystallographic characterization was done by using Transmission electron microscopy (TEM), High resolution transmission electron microscopy (HRTEM) and corresponding selected area electron diffraction (SAED) pattern by using TECNAI F20 Philips, operating at an acceleration voltage 200 kV. The photoelectrochemical measurement was carried out by irradiating the photoanode (TiO₂) with UV light recorded at electrochemical workstation AUTOLAB PGSTAT100 potentiostat. The photoelectrochemical cell was a two electrode system: TiO₂ film as a working electrode with active surface area of 1 cm², Graphite as a counter electrode and 0.1M NaOH as an electrolyte illuminated by 5mW/cm² intensity UV source. The charge recombination properties and electron transport resistance of TiO₂ microflowers were investigated by

electrochemical impedance measurements (model: AUTOLAB PGSTAT100 potentiostat) in frequency range 0.1 - 10⁵ Hz.

Results and Discussion

Formation Mechanism

The growth of hybrid nanostructured TiO₂ microflowers takes place by formation of Titanium glycolate complex via hydrothermal treatment. The Ti species initially react with ethylene glycol (EG) to form large molecular network by complexation between EG and Ti species to form, [Ti(OC₃H₇)_m(OC₂H₄OH)_{6-m}]^(4-m) species. In this reaction process (OC₂H₄OH)⁻ as a barrier to control the hydrolysis rate of Ti(OC₃H₇)₄ in water. At high temperature and pressure condition hydrolysis was accelerated to form [Ti(OH)_n(OC₃H₇)_m(OC₂H₄OH)_{6-n-m}]^(4-n+m) species leading to nucleation which is advantageous for further growth. Then the addition of CTAB enhances the surface morphology. After addition of CTAB the hydrogen atom of the OH group can be substituted with cationic head group of CTAB which results in the formation of spherical composite consisting micelle [34]. The role of hydrochloric acid to make the Ti species be charged leads to electrostatic repulsion between charged [Ti(OH)_n(OC₃H₇)_m(OC₂H₄OH)_{6-n-m}]^(4-n+m) species which is beneficial for the formation of microflowers like structure. [35, 36].



Scheme 1 schematic representation of growth route of hybrid structured TiO₂ microflowers.

Optical Study

The band gap energy (E_g), type of transition and absorption coefficient (α) of TiO₂ thin films were determined from optical absorption spectra shown in Fig.1. The optical absorption of S₁- S₅ samples shown in Fig.1 indicates absorption lies mainly in UV region due to its wide band gap (3.02 eV). The strong UV absorption of TiO₂ sample is due to electronic transition of electron from valance band to conduction band. The absorption coefficient can be expressed by equation (1),

$$\alpha h\nu = a(h\nu - E_g)^n \dots\dots\dots (1)$$

Where,

α is absorption coefficient, $h\nu$ is Photon Energy
 E_g is band gap energy, A is constant

The exponent 'n' depends on nature of transition during absorption process. For direct allowed transition $n = 1/2$ and for indirect allowed transition $n = 2$. The band gap energy can be

estimated by extrapolating straight portion of $(\alpha h\nu)^{1/2}$ versus photon energy ($h\nu$) shown in inset of Fig. 1 indicating indirect and allowed optical transition.

The band gap energy determined and it varies between 2.89- 2.94 eV for samples S_1 - S_5 respectively thus there is no remarkable change is observed in band gap of TiO_2 upon addition of CTAB.

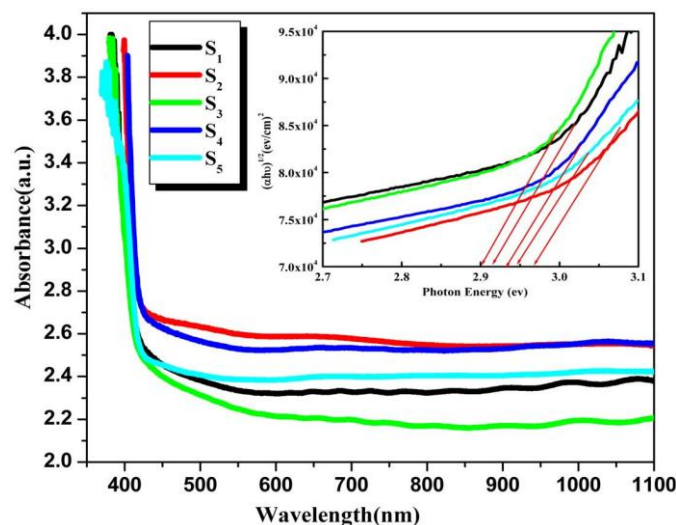


Fig.1: Absorbance spectra of hybrid structured TiO_2 microflowers (S_1 - S_5) inset of figure shows optical absorption spectra of the same.

Structural Analysis

X- Ray Diffraction (XRD)

The XRD pattern of 3D hierarchical hybrid structured TiO_2 microflowers shown in Fig.2. From XRD, the 2θ values 27.70° , 36.22° , 41.35° , 54.58° and 56.97° assigned to (110), (101), (111), (211), and (220) crystal planes of TiO_2 . All the peaks observed in XRD are indexed to Tetragonal rutile phase of TiO_2 with lattice constant $a=4.5570\text{\AA}$ and $c=2.9457\text{\AA}$ which is well agreement with standard Space Group: P 42/ mmm, JCPDS: 00 001-0562.

Table.1 Lattice parameters of hybrid structured TiO_2 microflowers prepared at different CTAB concentration.

Sample	Crystallite size (nm)	Lattice parameters (observed) (\AA)		Lattice parameters (Standard) (\AA)	
		a	c	a	c
S_1	39	4.5716	2.9410		
S_2	30	4.5814	2.9513		
S_3	28	4.5895	2.9536	4.5925	2.9578
S_4	27	4.5570	2.9457		
S_5	23	4.5781	2.9500		

The presence of highly intense, well defined and sharp peaks indicates good crystallinity of the samples. The other peaks observed in XRD which are originated from FTO substrate. The XRD pattern of TiO_2 thin films shows no difference in the peak orientation. This indicates that on increase in surfactant concentration there is increase in intensity of reflection. Average crystallite size of TiO_2 sample were calculated by using Scherrer's formula shown in equation (2),

$$D = \frac{0.94\lambda}{\beta \cos \theta} \quad \dots\dots\dots (2)$$

Where,

θ is Peak position of X-ray diffraction,

β is Full Width at Half Maxima (FWHM) of (110) plane for rutile TiO_2 in radian.

λ is Wavelength of X-ray used (0.154 nm)

The calculated crystallite size of TiO_2 for (110) planes are found to be 39, 30, 28, 27 and 23 nm for S_1 – S_5 samples respectively, such crystalline nature suppress the electron hole pair recombination which is beneficial for enhancement in the PEC performance. The * symbol indicates the presence of peak due to FTO substrate.

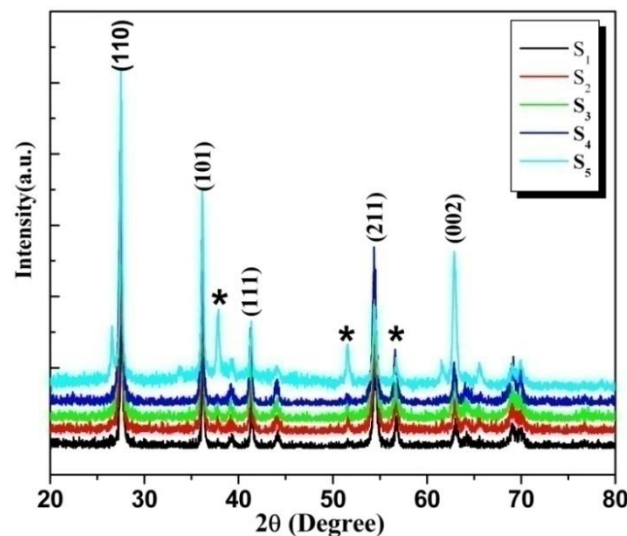


Fig.2 X-ray Diffraction (XRD) pattern of hybrid structured TiO_2 microflowers in the diffraction angle range (2θ) 20° - 80° .

High Resolution Transmission Electron Microscopy (HRTEM)

Crystallographic characterization of hybrid structured TiO_2 microflowers was performed using transmission electron microscopy (TEM) shown in Fig 3 (a).

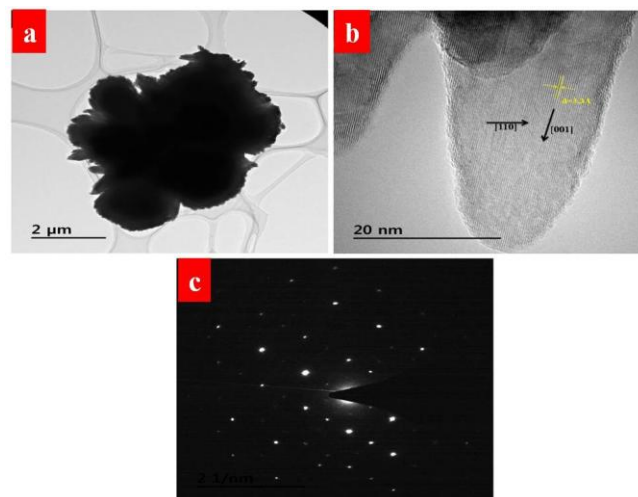


Fig.3 (a) Transmission electron microscopy (TEM), (b) High resolution transmission electron microscopy (HRTEM) image, (c) Selected area electron diffraction (SAED) pattern of hybrid structured TiO_2 microflowers.

The basic unit of TiO_2 is made up of nanorods as building blocks assembled to form microflowers with length $1.5\mu\text{m}$ and diameter $5\mu\text{m}$ which is well agreement with SEM results. HRTEM (fig.3 b) study illustrate that the TiO_2 microflowers possess a single crystalline structure of rutile TiO_2 with lattice spacing $d_{110} = 3.3\text{\AA}$ indicating the growth along [110] crystal plane with preferred [001] orientation it is well indexed with XRD results [37]. The [110] plane is thermodynamically stable plane so; the growth rate along this plane is faster than that of the other planes [38]. Fig.3 (b) indicates that the microflower is made from numerous nanorods having average diameter 25 nm. The TEM observation is consistent with the XRD results.

SAED pattern shown in fig. 3(c) manifests that TiO_2 microflowers are not aggregation of small crystallites but made up of monocrystal nanorods growing homocentrically. HRTEM and corresponding SAED pattern confirms single crystalline nature of TiO_2 microflowers and the enhanced photoelectrochemical performance

can be attributed to improved charge-separation by superior charge transportation through single-crystalline 3D TiO_2 microflowers.

Morphological Analysis

Scanning Electron Microscopy (SEM) Study

Fig.4 shows top view and cross sectional view of scanning electron microscopy (SEM) images for $S_1 - S_5$ samples of hierarchical hybrid structured TiO_2 microflowers on FTO substrate prepared by a simple single step hydrothermal method. In preliminary the TiO_2 thin films were synthesized without CTAB surfactant (sample S_1) and in order to investigate the effect of CTAB surfactant on morphology, the concentration of CTAB was varied from 0.025-0.15% (S_2-S_5).

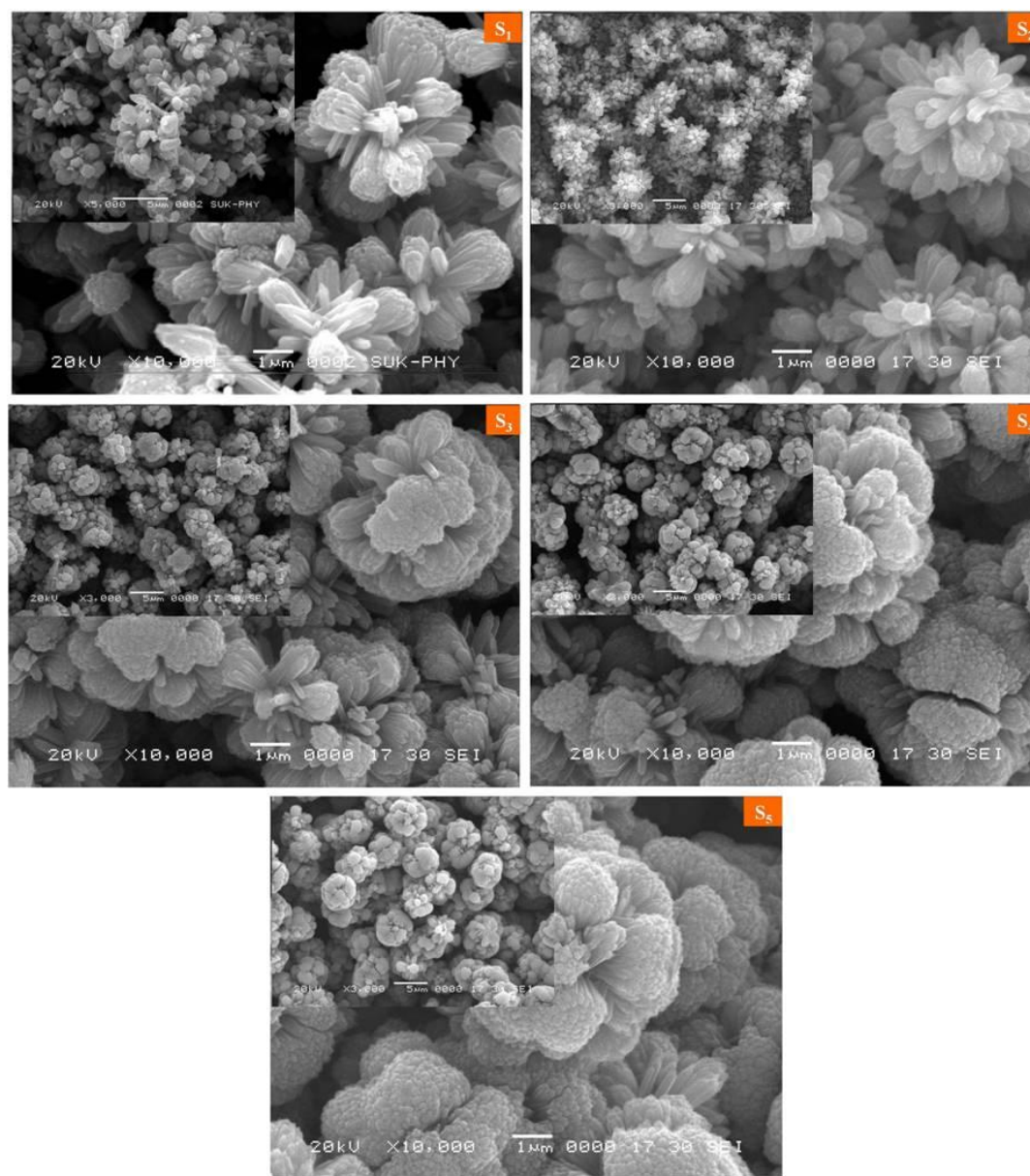


Fig.4 (a) Scanning electron microscopy (SEM) of hybrid structured TiO_2 microflowers, inset figure shows low magnification SEM image.

The SEM study manifests that the shape of microflowers changes significantly from samples S_1 to S_5 . By increasing concentration of CTAB the length, diameter and degree of aggregation of nanorods are increased and formation of microflowers takes place by nanorods growing homocentrically. In case of sample S_1 there is formation of incompletely grown microflower while as the surfactant concentration increases well defined microflowers were formed. Such microflowers are made from numerous nanorods display open structure, extended outside and become gradually compact inside [39-41].

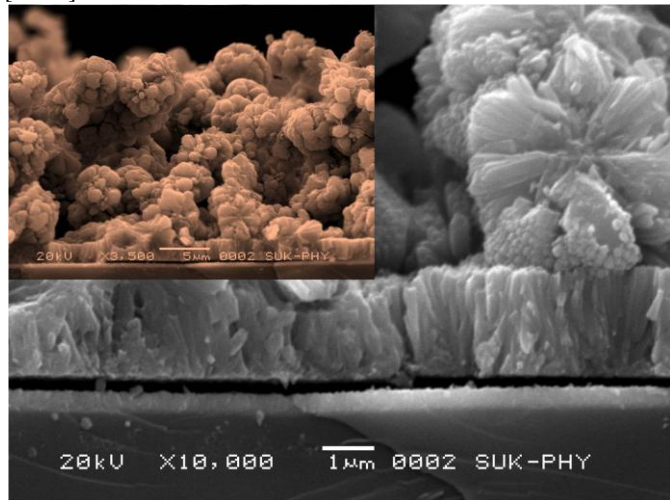


Fig.4 (b) Cross sectional view of hybrid structured TiO_2 microflowers.

The cross sectional view of the sample S_4 fig. (4b) showing that the obtained material is made from two parts, the upper part is made from microflowers with diameter $5\ \mu\text{m}$ while the lower part is made from nanorods nearly perpendicular to FTO with $1.5\ \mu\text{m}$ length. Most of nanorods are densely packed in to bundles. The 1D nanorods can accelerate the movement of electron in one direction while 3D hierarchical microflowers being used as a scattering layer and it can enhance the cell performance by light harvesting. Therefore, double layered structure with scattering layer has been widely used to improve the conversion efficiency of solar cell. It is also observed that there is good connection between microflowers and nanorods which strengthened the interpartical connection offering abundant transfer pathway for photogenerated electrons improving the solar cell performance.

Energy Dispersive Spectroscopy [EDS]

Chemical composition of pure TiO_2 estimated by energy dispersive spectroscopy [EDS] shown in Fig.5. The EDS spectrum shows prominent peak of titanium [Ti] and oxygen [O]. From the EDS pattern it is confirmed that, TiO_2 microflowers synthesized by hydrothermal method belong to pure TiO_2 (1:2).

X-ray Photoelectron Spectroscopy (XPS)

The elemental composition and valance state of elements present in the material was determined by XPS spectra shown in Fig.6. The XPS survey spectrum fig.6 (a) indicates the presence of Ti, O and also C elements.

The presence of carbon at binding energy $284.05\ \text{eV}$ was due to surface contamination when TiO_2 thin film was exposed to

atmosphere. The core level spectrum of Ti 2p fig.6 (b) shows peak at binding energy $464.27\ \text{eV}$ and $458.49\ \text{eV}$ attributed to Ti $2p_{1/2}$ and Ti $2p_{3/2}$ respectively. The energy difference between Ti $2p_{1/2}$ and Ti $2p_{3/2}$ peak was found to be $5.78\ \text{eV}$ which corresponds to Ti^{4+} state of Titanium in rutile TiO_2 which is well agreement with standard value [44].

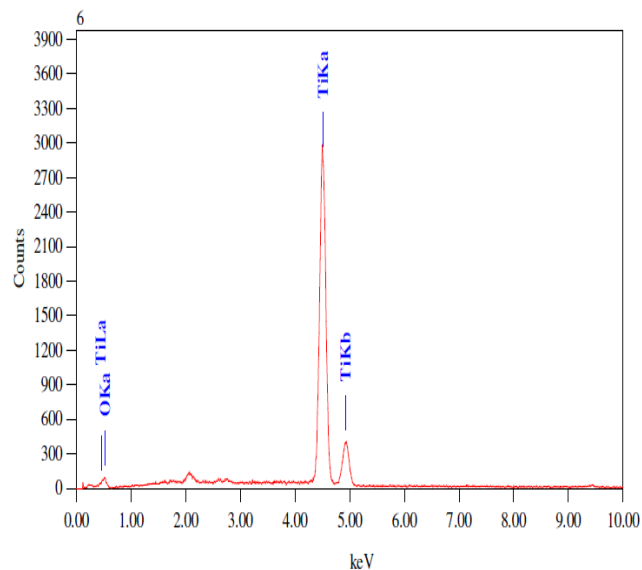


Fig.5 Energy dispersive spectroscopy (EDS) of hybrid structured TiO_2 microflowers.

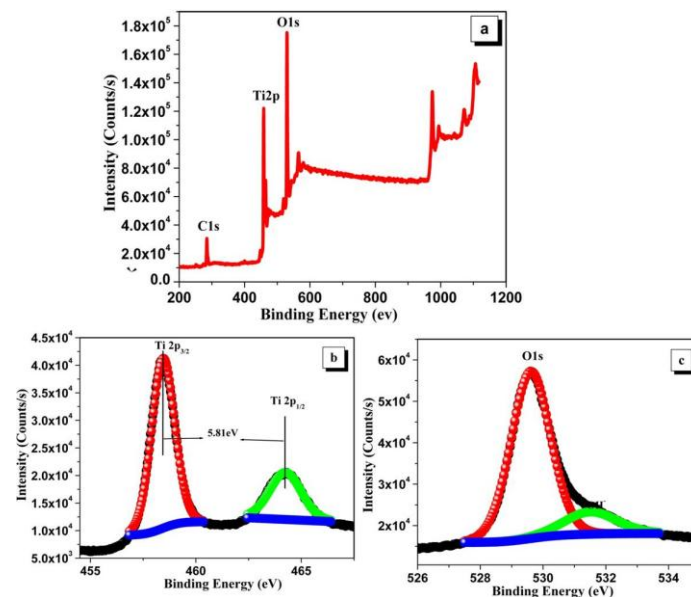


Fig.6 X-ray photoelectron spectroscopy (XPS) for TiO_2 microflowers [a] Survey spectrum of TiO_2 [b] core level spectrum of Ti 2p [c] core level spectrum of O 1s.

The high resolution scan of O 1s peak shown in fig.6 (c) can be deconvoluted into two peaks at binding energy $529.58\ \text{eV}$ and $531.52\ \text{eV}$ respectively. The peak at binding energy $529.58\ \text{eV}$ corresponds to lattice Oxygen (O-Ti-O) and latter is related to hydroxyl group (OH) adsorbed during transfer.

Photoelectrochemical (PEC) Performance

Fig.7 demonstrates the photocurrent density versus the voltage plot recorded by using linear sweep voltamogram with two electrodes system illuminated under 5 mW/cm² UV light. The cell configuration used to record the *J*-*V* curve is as follows,

Glass / FTO/ TiO₂ / 0.1M NaOH / G

The photoelectric performance i.e. Fill Factor (FF) and overall light to electric energy conversion efficiency ($\eta\%$) was calculated by equations (3) and (4) respectively as follows,

$$FF = \frac{J_{\max} V_{\max}}{J_{sc} V_{oc}} \quad \dots\dots\dots (3)$$

Where,

V_{oc} is open circuit voltage,

J_{sc} is short circuit current density,

V_{\max} is maximum voltage,
 J_{\max} is maximum current density.

$$\eta(\%) = \frac{J_{sc} V_{oc}}{P_{in}} \times FF \times 100 \quad \dots\dots\dots (4)$$

The solar cell based on hierarchical hybrid structured TiO₂ photoanode gives a short circuit current density (J_{sc}) 0.113 mA/cm², open circuit voltage (V_{oc}) 383 mV and fill factor (FF) 0.28 yields a power conversion efficiency ($\eta\%$) is 0.23% for 'S₁' sample. Effective enhancement in the photoelectrochemical performance is observed with increase in CTAB concentration.

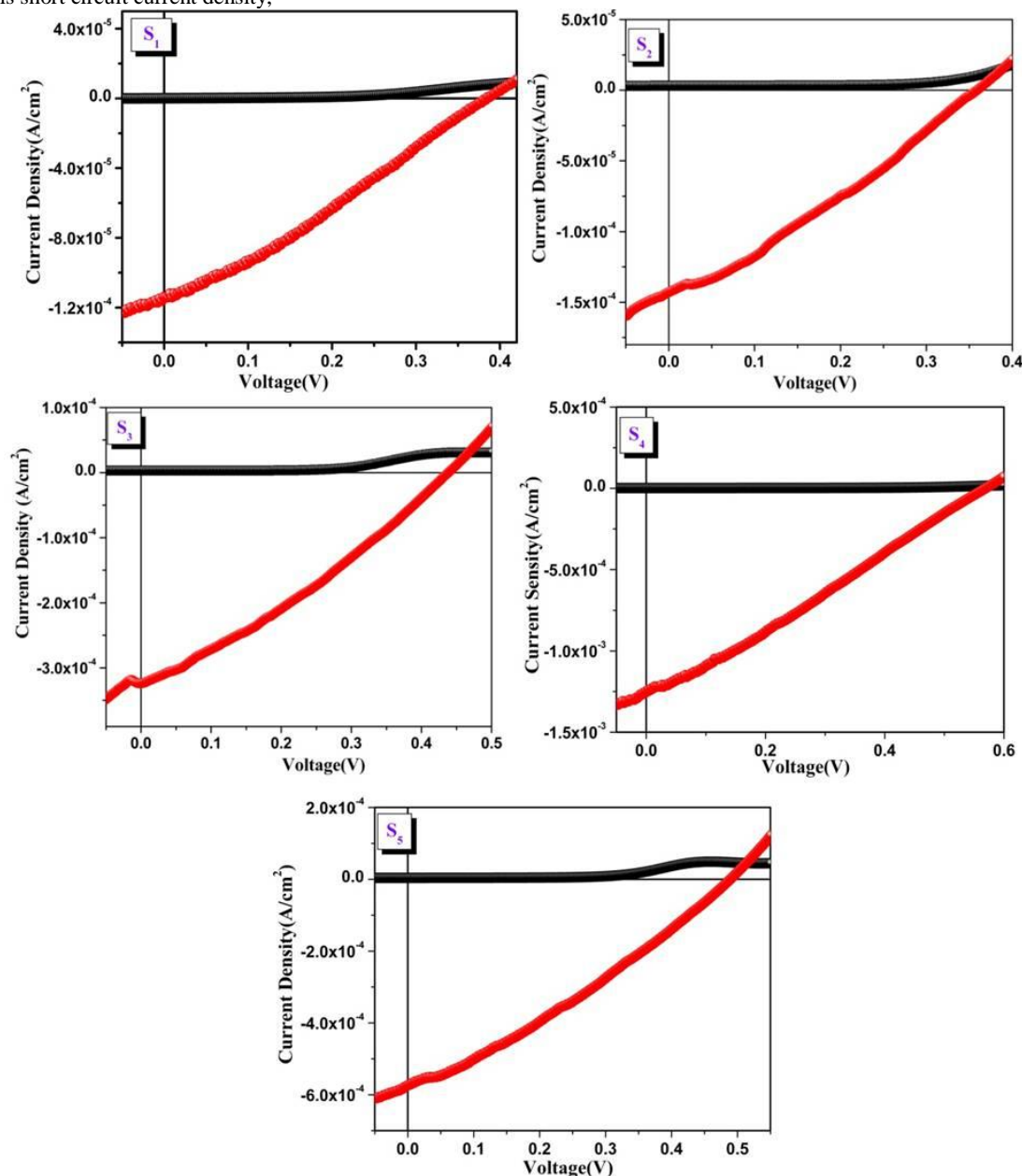
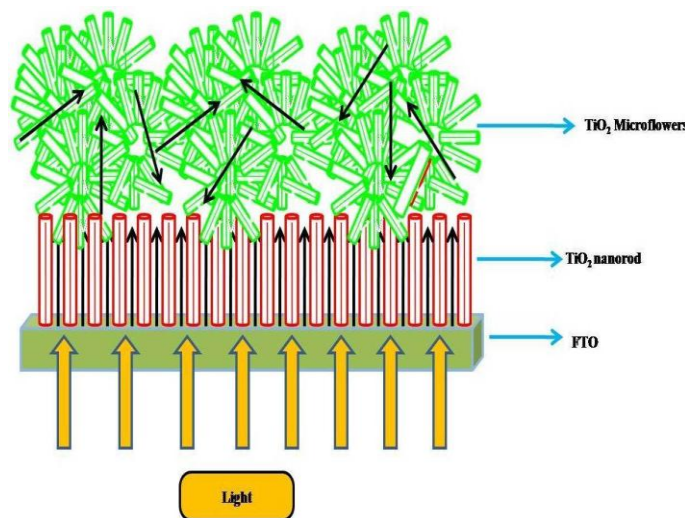


Fig.7 Photoelectrochemical (PEC) performance of hierarchical hybrid structured TiO₂ microflowers.

Electrodes	V_{oc} (mV)	J_{sc} (mA/cm ²)	V_{max} (mV)	J_{max} (mA/cm ²)	FF	η (%)	R_s (Ω)	R_{sh} (Ω)
S ₁	219	0.113	219	0.054	0.27	0.23	2367.6	3567.86
S ₂	357	0.142	184	0.082	0.29	0.29	1341.18	3539.82
S ₃	433	0.323	251	0.173	0.31	0.86	1152.00	10365.00
S ₄	573	1.255	313	0.609	0.26	3.72	471.76	571.42
S ₅	487	0.568	301	0.279	0.30	1.18	550.00	649.77

Table.2 Photovoltaic measurements of hybrid structured TiO₂ microflowers based photoanode.

As the CTAB concentration is 0.1% for sample S₄ the photocurrent density increases up to 1.255 mA/cm², V_{oc} is 573 mV and FF is 0.26 giving rise to 3.72% power conversion efficiency. There is sharp increase in photovoltaic performance from sample S₃ to S₄. This is because in case of sample S₃ the unabsorbed light penetrates through nanorods without being scattered for the improvement in PEC performance but for samples S₄ the microflowers are assembled with nanorods to form microflowers causes scattering of incident light many times for better photoconversion efficiency i.e. 3.72%.



Scheme 2 Light travelling path in the photoelectrode based on TiO₂ nanorods and TiO₂ microflowers as a light scattering layer.

Such improvement in conversion efficiency can be explained on the basis of surface modification by CTAB. The improvement in the energy conversion is due to bilayered structure of TiO₂ in which 3D microflowers can act as a scattering overlayer and 1D nanorods underlayer. The 1D nanorods can accelerate the movement of electron in one direction while 3D hierarchical microflowers being used as a scattering layer and it can enhance the cell performance by light harvesting [45- 48]. The microflowers forms a compact layer, which favours the accumulation of electrons at the TiO₂/FTO interface resulting shifting its potential to higher value.

As the concentration of CTAB increased above 0.1% (sample S₅) the rods are densely packed into bundles. Due to formation of densely packed bundles on the surface less scattering of light takes

place which results into decrease in the power conversion efficiency. Due to that reason sample S₅ possesses low photoconversion efficiency i.e. 1.18%. Thus, the effect of surfactant on the photoelectrical performance was summarized in the Table.2.

The series resistance (R_s) and shunt resistance (R_{sh}) were examined from J - V curve using equations (5) and (6) respectively as follows,

$$\left(\frac{dI}{dV}\right)_{I=0} = \frac{1}{R_s} \dots\dots\dots (5)$$

$$\left(\frac{dI}{dV}\right)_{V=0} = \frac{1}{R_{sh}} \dots\dots\dots (6)$$

The ideal solar cells have R_{sh} value approaching infinity and R_s near zero. The variation in R_s and R_{sh} summarized in the Table.2 and R_s and R_{sh} varies from 471.76 to 2367.6 Ω and 571.42 to 10365 Ω respectively for sample S₁-S₅. High value R_{sh} of the material shows no shorts of current in circuit and low value R_s gives high current flow through the circuit. Thus the monotonic increase in open circuit voltage (V_{oc}) due to less resistance to electron transfer and reduction in charge recombination rate. These voltage characteristics largely dependent on shunt resistance (R_{sh}) and series resistance (R_s).

Electrochemical Impedance (EIS) Measurement

Electrochemical impedance is a powerful steady-state technique used to measure the ability of circuit to resist to the flow of electric current. In typical impedance spectra we observed three electric arcs in the frequency range 10³ - 10⁵ Hz corresponds to the resistance at FTO conducting layer / TiO₂ interface, 1 - 10³ Hz and 0.1 - 1 Hz have been assigned to the resistance at TiO₂ / Electrolyte interface and counter electrode / electrolyte respectively.

Fig.8 shows Nyquist plots for samples S₁-S₅, measured under 0.6 V open circuit voltage in dark and frequency range is from 0.1 - 10⁵ Hz. The equivalent circuit model fitted to the value is shown in inset of fig. 8. The equivalent circuit consists of various components: ohmic series resistance [R_s], charge transfer resistance at counter electrode / Electrolyte interface (R_1), charge transfer resistance at TiO₂ photoanode / electrolyte interface (R_2), constant phase capacitance corresponds to R_1 and R_2 are CPE₁ and CPE₂ respectively and fitted values are listed in the Table.3

Electrochemical impedance study reveals that at lower series resistance for sample S₄ (85.3 Ω cm⁻²) which favours the injection of more electrons to the TiO₂ photoanode and thereby raising the Fermi

level of the TiO₂ photoanode and thus shifting its potential to higher value causes enhancement in the photoconversion efficiency.

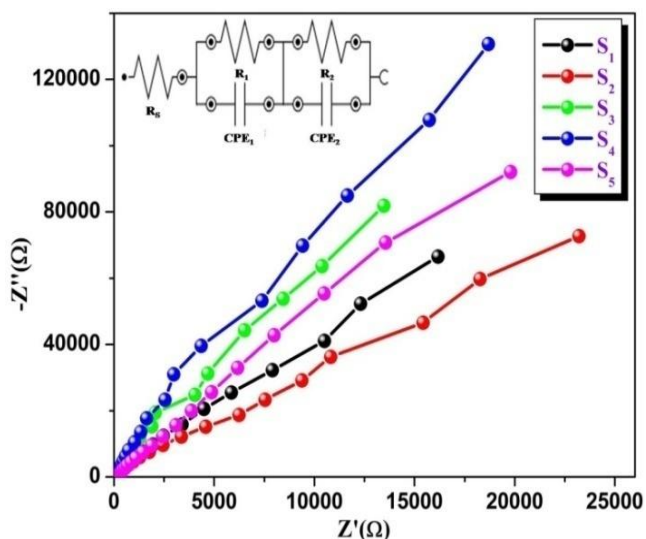


Fig.8 Electrochemical impedance (EIS) measurement for hybrid structured TiO₂ microflowers, inset of the fig shows equivalent circuit employed to fit impedance data.

EIS study suggests that the electric arcs for sample S₁-S₅ at high frequency region and the electron concentration in TiO₂ is low due to frequent recombination, referable to reason that efficiency of TiO₂ is limited. The EIS measurement reveals that the impedance of both the electrochemical reaction at counter electrode (R₁) and the charge transfer at TiO₂ photoanode / electrolyte interface (R₂) decreases with surface modification by CTAB. The substantial reduction in resistance mainly ascribed to the improvement in the electron transport. Thus, the sample S₄ has R₁=1020 Ωcm⁻² and R₂= 3770 Ωcm⁻² which shows lower resistance than that of other samples. Lower the resistance to the flow photogenerated charge carriers adventitious for higher conversion efficiency.

becomes gradually compact inside. The 3D hierarchical microflowers can act a scattering overlayer while the 1D nanorods underlayer. By using this underlayer and overlayer built from nanorod and microflowers, TiO₂ photoanode was constructed. The microflowers forms a compact layer, which favours the accumulation of electrons at the TiO₂/FTO interface resulting shifting its potential to higher value. The increase in CTAB concentration (S₁-S₅) results into increase in power conversion efficiency from 0.23 % - 3.72 %. The monotonic increase in power conversion efficiency is due to less resistance to electron transfer and reduction in charge recombination rate. As well EIS study demonstrated that, lower series resistance (85.3 Ωcm⁻²) is favourable for injection of more electrons to the TiO₂ photoanode causes rising in Fermi energy level of the TiO₂ photoanode. The overall study signifies that, the formation of hybrid structured TiO₂ microflowers is highly useful for enhancement in power conversion efficiency due to high crystallinity, well-interconnected compact layer and scattering phenomenon.

Acknowledgement

One of the authors PBP thankful to UGC New Delhi for providing financial support through scheme of Sciences for Meritorious Students and authors VVK wishes to acknowledge the DAE-BRNS Mumbai for financial support through DAE-BRNS project (2012/34/51/BRNS/2036). This work was also supported by the Priority Research Centre Program through the National Research Foundation of Korea (NRF) funded by the Ministry of Education, Science and Technology (2009-0094055)

Notes and references

^aMaterials Research Laboratory, Department of Chemistry, Shivaji University, Kolhapur-416004, India.

^bThin Film Materials Laboratory, Department of Physics, Shivaji University, Kolhapur-416004, India.

^cPolymer Energy Materials Laboratory, Department of Advanced Chemical Engineering, Chonnam National University, Gwangju, South Korea.

*Corresponding Author: p_n_bhosale@rediffmail.com, Tel Number: 091-231-2609338, Fax: +91-231-2691533 (O).

- 1) S. K. Balasingam, M. G. Kang and Y. Jun, *Chem. Commun.*, 2013, **49**, 11457.
- 2) D. P. Singh, A. George, R.V. Kumar, J.E. ten Elshof, and M. Wagemaker *J. Phys. Chem. C*, 2013, **117**, 19809.
- 3) Z. He and W. Que, *Phys. Chem. Chem. Phys.*, 2013, **15**, 16768.
- 4) V. Müller and P. Schmuki, *Electrochem. Commun.*, 2014, **42**, 21.
- 5) Z. Zhao, H. Tan, H. Zhao, D. Li, M. Zheng, P. Du, G. Zhang, D. Qu, Z. Sun and H. Fan, *Chem. Commun.*, 2013, **49**, 8958.
- 6) Z. Penga, Y. Liua, Y. Zhaoa, W. Shua, K. Chena, Q. Baob and W. Chena, *Electrochim. Acta*, 2013, **111**, 755.
- 7) X. Song, M. Wang, Y. Shi, J. Deng, Z. Yang and X. Yao, *Electrochim. Acta*, 2012, **81**, 260.
- 8) S. Kim, M. Son, S. Park, M. Jeong, K. Prabakar and H. Kim, *Electrochim. Acta*, 2014, **118**, 118.
- 9) L. Zhua, Y.L. Zhaoa, X.P. Lina, X.Q. Gua and Y.H. Qianga, *Superlattices Microstruct.*, 2014, **65**, 152.
- 10) L. Fenga, J. Jiaa, Y. Fangb, X. Zhoub and Y. Linb, *Electrochim. Acta*, 2013, **87**, 629.
- 11) E. Y. Kima, S. Yua, J. H. Moona, S. M. Yooa, C. Kimb, H. K. Kim and W. I. Leea, *Electrochim. Acta*, 2013, **111**, 261.
- 12) P. Sun, X. Zhang, C. Wang, Y. Wei, L. Wang and Y. Liu, *J. Mater. Chem. A*, 2013, **1**, 3309.
- 13) V.V. Divya Rani, R. Ramachandran, K. P. Chennazhi, H. Tamura, S.V. Nair and R. Jayakumar, *Carbohydr. Polym.*, 2011, **83**, 858.
- 14) Y. Qu, W. Wang, L. Jing, S. Song, X. Shi, L. Xue and H. Fu, *Appl. Surf. Sci.*, 2010, **257**, 151.

Electrode	R _s (Ωcm ⁻²)	R ₁ (Ωcm ⁻²)	CPE ₁ (μF)	R ₂ (Ωcm ⁻²)	CPE ₂ (μF)
S ₁	89.0	1410	21.2	2350	18.4
S ₂	107	4970	9.80	2630	36.4
S ₃	98.5	8440	28.9	9440	15.5
S ₄	85.3	1020	9.00	3770	13.8
S ₅	173	2110	29.5	4180	19.5

Table.3 Values of Resistance (R) and Capacitance (CPE) observed in equivalent circuit shown in inset of Fig. 8

Conclusion

In this study the, surfactant directed single step facile hydrothermal technique was implemented to form better interconnecting network of TiO₂ microflowers for boosting the photoelectrochemical performance. Different CTAB concentration reveals the formation of nanorods assembled microflowers with different length, diameter and degree of aggregation with high crystallinity contribute positively in photoelectrochemical performance. The SEM study manifests that microflowers are made from numerous nanorods growing homocentrally, display open structure, extended outside and

- 15) A. Kafizas, C. W. Dunnill and I. P. Parkin, *Phys. Chem. Chem. Phys.*, 2011, **13**, 13827.
- 16) S. Segota, L. Curkovic, D. Ljubas, V. Svetlic, I. F. Houra and N. Tomas, *Ceram. Int.*, 2011, **37**, 1153.
- 17) J. Zhang, S. Li, H. Ding, Q. Li, B. Wang, X. Wang and H. Wang, *J. Power Sources*, 2014, **247**, 807.
- 18) Z. Su and W. Zhou, *J. Mater. Chem.*, 2011, **21**, 8955.
- 19) A. A. Ismail and D. W. Bahnemann, *J. Mater. Chem.*, 2011, **21**, 11686.
- 20) J. Zhang, S. Li, H. Ding, Q. Li, B. Wang, X. Wang and H. Wang, *J. Power Sources*, 2014, **247**, 807.
- 21) M. Kim, C. Bae, H. Kim, H. Yoo, J. M. M. Moreno, H. S. Jung, J. Bachmann, K. Nielsch and H. Shin, *J. Mater. Chem. A*, 2013, **1**, 14080.
- 22) W. Zhou, X. Liu, J. Cui, D. Liu, J. Li, H. Jiang, J. Wang and Hong Liu, *Cryst. Eng. Comm*, 2011, **13**, 4557
- 23) J. S. Chen, Y. N. Liang, Y. Li, Q. Yan and X. Hu, *Appl. Mater. Interfaces*, 2013, **5**, 9998.
- 24) T. Zeng, H. Tao, X. Sui, X. Zhou and X. Zhao, *Chem. Phys. Lett.*, 2011, **508**, 130.
- 25) T. A. Arun, A. A. Madhavan, D. K. Chacko, G. S. Anjusree, T. G. Deepak, S. Thomas, S. V. Nair and A. S. Nair, *Dalton Trans.*, 2014, **43**, 4830.
- 26) D. Li, M. Carette, A. Granier, J.P. Landesman and A. Goulet, *Thin Solid Films*, 2012, **522**, 366.
- 27) H. Liua, Y. Zhanga, R. Li, M. Cai and X. Suna, *J. Colloid Interface Sci.*, 2012, **367**, 115.
- 28) C. Jiang, M. Y. Leung, W. L. Koh and Y. Li, *Thin Solid Films*, 2011, **519**, 7850.
- 29) S.S.Mali, H.Kim, C.S.Shim, P.S.Patil, J. H. Kim, and C. K. Hong, *Sci. Rep.* 2013, **3**, 3004.
- 30) Y. Park, Y. Chang, B. Kum, E. Kong, J. Y. Son, Y. S. Kwon, T. Park and H. M. Jang, *J. Mater. Chem.*, 2011, **21**, 9582.
- 31) J. Jiang, F. Gu, W. Shao and C. Li, *Ind. Eng. Chem. Res.*, 2012, **51**, 2838.
- 32) H. Koo, Y. J. Kim, Y. H. Lee, W. I. Lee, K. Kim and N. Park, *Adv. Mater.*, 2008, **20**, 195.
- 33) S. R. Gajjela, C. Yapa and P. Balaya, *J. Mater. Chem.*, 2012, **22**, 10873.
- 34) S. Gea, B. Wang, D. Li, W. Fa, Z. Yang, Z. Yang, G. Jia and Z. Zheng, *Appl. Surf. Sci.*, 2014, **295**, 123.
- 35) H. Zhang, H. Yu, Y. Han, P. Liu, S. Zhang, P. Wang, Y. Cheng and H. Zhao, *Nano Res.*, 2011, **4**, 938.
- 36) Y. Duana, N. Fua, Y. Fang, X. Li, Q. Liu, X. Zhou and Y. Lin, *Electrochim. Acta*, 2013, **113**, 109.
- 37) H. Pang, H. Yang, C. X. Guo, J. Lua and C. M. Li, *Chem. Commun.*, 2012, **48**, 8832.
- 38) W. Zhou, X. Liu, J. Cui, D. Liu, J. Li, H. Jiang, J. Wang and H. Liu, *Cryst. Eng. Comm*, 2011, **13**, 4557.
- 39) F. Shao, J. Sun, L. Gao, S. Yang and J. Luo, *Appl. Mater. Interfaces*, 2011, **3**, 2148.
- 40) X. Tan, P. Qiang, D. Zhang, X. Cai, S. Tan, P. Liu and W. Mai, *Cryst. Eng. Comm*, 2014, **16**, 1020.
- 41) Z. He, J. Liu, J. Miao, B. Liu and T. T. Y. Tan, *J. Mater. Chem. C*, 2014, **2**, 1381.
- 42) Y. Rui, Y. Li, Q. Zhang and H. Wang, *Cryst. Eng. Comm*, 2013, **15**, 1651.
- 43) D. We, Y. Wang, H. Dong, F. Zhu, S. Gao, K. Jiang, L. Fu, J. Zhang and D. Xu, *Nanoscale*, 2013, **5**, 324.
- 44) V. V. Kondalkar, S. S. Mali, N. B. Pawar, R. M. Mane, S Choudhury, C. K. Hong, P. S. Patil, S. R. Patil P. N. Bhosale and J. H. Kim *Electrochim. Acta*, 2014, **143**, 89.
- 45) S. S. Mali, H. Kim, C. S. Shim, W. R. Bae, N. L. Tarwal, S. B. Sadale, P. S. Patil, J. H. Kim and C. K. Hong, *Cryst. Eng. Comm*, 2013, **15**, 5660.
- 46) P. Cheng, S. Du, Y. Cai, F. Liu, P. Sun, J. Zheng and G. Lu, *J. Phys. Chem. C*, 2013, **117**, 24150.
- 47) H. S. Kim, Y. J. Kim, W. Lee and S. H. Kang, *Appl. Surf. Sci.*, 2013, **273**, 226.
- 48) S. S. Mali, P. S. Shinde, C. A. Betty, P. N. Bhosale, W. J. Lee and P. S. Patil, *Prog. Photovolt: Res. Appl.*, 2014, **22**, 525.